GEOPHYSICS

Shear properties of Earth's inner core constrained by a detection of *J* waves in global correlation wavefield

Hrvoje Tkalčić* and Thanh-Son Phạm

Seismic *J* waves, shear waves that traverse Earth's inner core, provide direct constraints on the inner core's solidity and shear properties. However, these waves have been elusive in the direct seismic wavefield because of their small amplitudes. We devised a new method to detect *J* waves in the earthquake coda correlation wavefield. They manifest through the similarity with other compressional core-sensitive signals. The inner core is solid, but relatively soft, with shear-wave speeds and shear moduli of 3.42 ± 0.02 kilometers per second and 149.0 ± 1.6 gigapascals (GPa) near the inner core boundary and 3.58 ± 0.02 kilometers per second and 167.4 ± 1.6 GPa in Earth's center. The values are 2.5% lower than the widely used Preliminary Earth Reference Model. This provides new constraints on the dynamical interpretation of Earth's inner core.

Earth's inner core was proposed more than 80 years ago to explain the arrival of compressional waves in places that were impossible to predict on the basis of the assumption of single-layered core (*1*). The hypothesis of a solid inner core is the result of the liquid-solid phase change in iron at high pressure (*2*), which implies the existence of shear waves in the inner core (seismic *J* phase). Previous claims of body-wave observations (*3*–*7*) featured bursts of energy around the time predicted by the spherically symmetric Preliminary Reference Earth Model (PREM) (*8*). The rigidity of the inner core in PREM is mainly constrained by Earth's free oscillations (*9*). However, *J* waves have remained elusive, because it was demonstrated that routine observations of *PKJKP* waves are extremely unlikely in the seismic wavefield at periods greater than 10 s (*10*). We used advances in earthquake coda cross-correlation (*11*) and identified the presence of the *J* phase. We identified arrivals of *PKJKP* waves in a correlation pair with another core phase, *PKIKPPKIKP* (hereafter referred to as *I2*), over a range of angular distances. This allowed us to determine, with high precision, the shear-wave speed reduction of 2.5 ± 0.5% relative to the reference model PREM, which corresponds to a shear-wave speed of 3.42 ± 0.02 km/s and shear modulus of 149.0 ± 1.6 GPa near the inner core boundary and 3.58 ± 0.02 km/s and 167.4 ± 1.6 GPa in Earth's center. This is evidence for a soft inner core and explains the absence of *PKJKP* waves in the seismic wavefield. Thus, our findings have a range of implications for the structure and dynamics of the inner core (*12*, *13*).

We have recently shown that the features emerging in the stacked cross-correlations (also known as Earth's cross-correlogram or global correlogram) do not correspond to structural Green's functions (response of Earth's structure between two receivers) but rather emerge owing to similarities of two or more seismic phases that arrive at recorders with the same slowness and share a common subset of propagation legs (*11*). Earth's correlation wavefield is thus a manifestation of similarity among seismic phases in the direct seismic wavefield (*14*). The similarity between the weak signals is a more efficient mechanism of detection than the identification of weak signals in the noisy seismic wavefield. Consequently, the correlation wavefield features "exotic seismic phases" that traverse Earth's inner core and deep parts of Earth, for example, multiple inner-core phases: *I3*, *I4*, and *I5*. Additionally, there are correlation phases that do not have correspondences in the direct seismic wavefield, for example, the phase *cS-cP*, which provides additional insights into the seismic wavefield (*11*, *14*).

We applied the above principles using global data (fig. S1) to conduct a systematic search for the presence of a *PKJKP* signal over a number of correlation pairs of seismic phases in which one of the phases is *PKJKP* (figs. S3 and S4). The rationale for this search is that the similarity of the reticent *PKJKP* signals with other, more prominent phases such as *PKiKP*, *PKIKP*, or *PKIKPPKIKP* (Fig. 1) will manifest itself as one of the features in the global correlogram. We successfully fit the travel-time prediction of three correlation phases: *PKIKPPKIKP-PKJKP* (*I2-PKJKP*), *PKIKP-PKJKP*, and *PKiKP-PKJKP*, with features in the global correlogram synthetized by the same Earth model (*14*). Because we observed *I2-PKJKP* near the angular distance 0°, the prominence occurs because of contributions from all azimuths (*15*). *PKIKP-PKJKP* and *PKiKP-PKJKP* are weaker because there is no such focusing effect in the 120° to 150° angular distance range (Fig. 2C).

Research School of Earth Sciences, The Australian National University, Canberra, ACT 2601, Australia.
*Corresponding author. Email: hrvoje.tkalcic@anu.edu.au

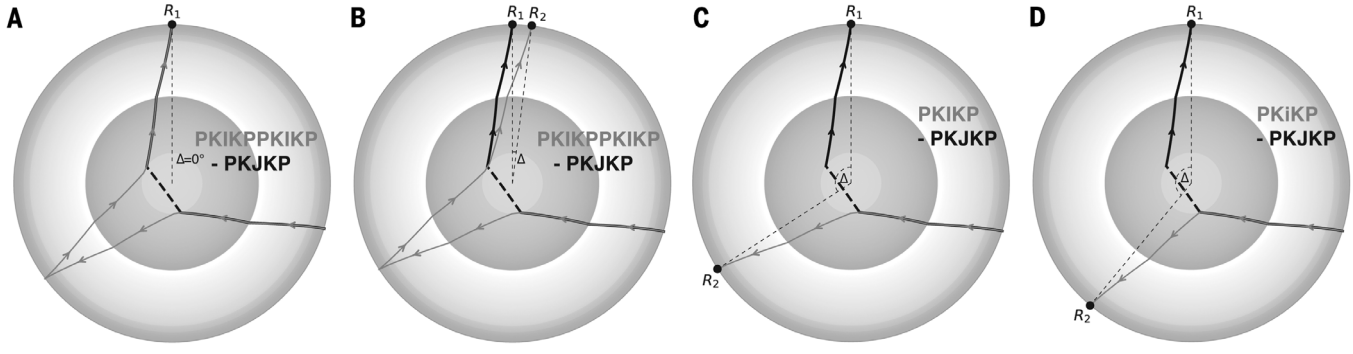

Fig. 1. Seismic phases, ray paths, and receiver geometry. (**A** to **D**) Cross sections of Earth illustrating the geometry of *PKJKP* waves and other compressional waves used to detect *PKJKP* in Earth's correlation wavefield. Shear-wave leg through the inner core is shown with a dashed line in all panels. The arrow indicates the direction of seismic waves. In (A), *PKJKP* is shown in black and *PKIKPPKIKP* in gray. *PKIKPPKIKP* is also referred to as *I2*. R_1 is the receiver at the angular distance Δ = 0° used to perform a cross-correlation. (B) is the same as (A), but the receivers are now separated by an angular distance Δ ≠ 0°. In (C), the two receivers are now separated by the angular distance Δ = 120°. PKJKP is shown in black and *PKIKP* in gray. (D) is similar to (C), but instead of *PKIKP* waves that traverse the inner core, the waves that correlate with *PKJKP* (black) are *PKiKP* waves that reflect from the inner core (gray). *PKJKP* is shown in black and *PKiKP* in gray.

We computed synthetic global correlograms for a crude parameter-space search over a range of shear-wave speed in the inner core (Fig. 2). Our synthesized global correlograms (Fig. 2) are, overall, insensitive to forced changes in the inner core shear-wave speed. We detected a number of prominent and stable features that correspond to the correlation phases (light blue curves). However, a clear move out (a shift in the time–angular distance domain) of *PKIKP-PKJKP*, *PKiKP-PKJKP*, and *I2-PKJKP* is evident with the changing inner core shear-wave speed. We compare these to the theoretically predicted arrivals that are based on the model PREM (orange curves). At the 10% reduction with respect to PREM (Fig. 2A), the *I2-PKJKP* cusp is visible, but there is a negative time offset with respect to the PREM prediction and the prominent phase *PcP** (*14*) that starts about a minute later at 15° of angular distance. With increased inner core shear-wave speed, the cusp shifted toward later times because *PKJKP* waves arrived earlier at the receiver, so that the time difference between *PKJKP* and later *I2* arrivals increases.

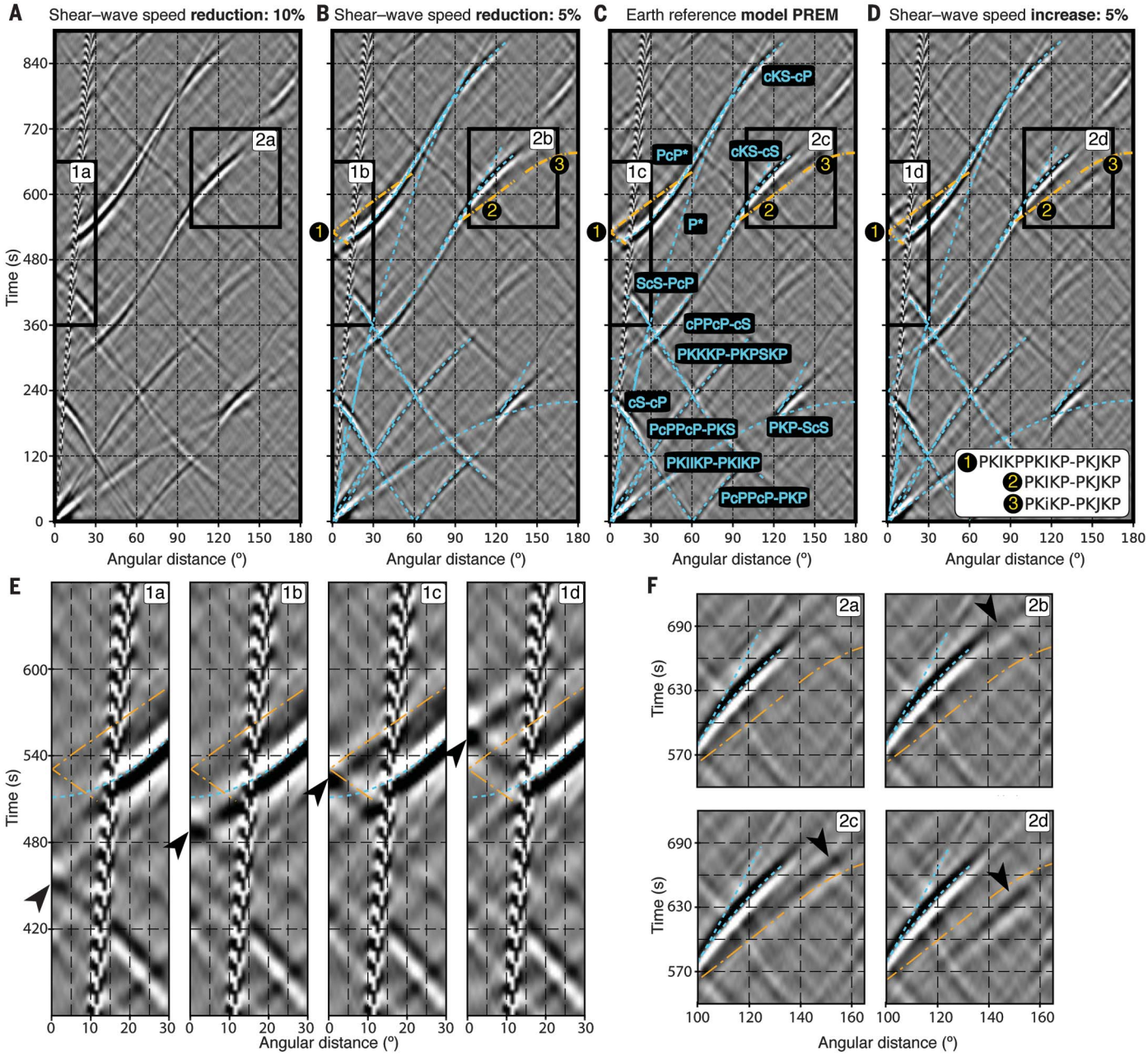

Fig. 2. Detection of *PKJKP* in synthetic correlation wavefield. (**A** to **F**) Synthetic global correlograms for different assumptions of shear-wave speed in Earth's inner core relative to the spherically symmetric Earth model PREM (*8*): (A) 10% reduction, (B) 5% reduction, (C) the PREM value (0% change), and (D) 5% increase. Windows 1 and 2 (indicated by the black rectangles) in (A) to (D) focus on the correlation phases of interest (indicated by yellow numbers 1, 2, and 3) and are enlarged in sections (E) and (F). Positive amplitudes are in white shades, and negative amplitudes are in black shades; the intensity of the black or white indicates the strength. Blue lines represent theoretically predicted features in the correlation wavefield that are insensitive to the inner core shear-wave speed; for clarity, they are labeled in (C) and omitted elsewhere. To enhance the clarity of all features, the theoretical curves are not shown in (A). Orange lines are theoretical predictions of *PKIKPPKIKP-PKJKP* (also called *I2-PKJKP*), *PKiKP-PKJKP*, and *PKIKP-PKJKP* according to the model PREM. For the ray geometry of these phases, see Fig. 1. Black arrows in (E) and (F) indicate the changing position of the features sensitive to the inner core shear-wave speed.

At the 5% increase, the cusp is more pronounced and is positioned upward with respect to the PREM prediction and the prominent phase *PcP** (Fig. 2D).

Our observed correlation wavefield is generally depleted in detail in comparison with the simulated correlation wavefield (*11*, *16*) (Fig. 3). However, the level of similarity that we reproduced through the seismic wavefield propagation in the spherically symmetric Earth model PREM in this frequency range (15 to 50 s) is notable. This attests to the generally well-constrained radial Earth model from long-period seismic observations. The *I2-PKJKP* cusp is a prominent feature that we identified in the observed correlation wavefield, whereas we cannot discern the *PKIKP-PKJKP* and *PKiKP-PKJKP*. We compared the *I2-PKJKP* cusp offset toward early times to the PREM prediction corrected by the dispersion relationship for the central period T = 23.1 s (*17*). Our fine parameter-space search simulations (*14*) yielded the best Earth model that fit the observed correlation wavefield, in which the inner core has a 2.5 ± 0.5% reduced shear-wave speed relative to the PREM values. We based our estimate on visual comparisons of the cusp positions and of negative peaks in the slant stacks produced from our observed and synthetized correlation wavefield (Fig. 3D). The width of the fringes of the features in the correlograms prevents a better estimate of their position at the present time. More-quantitative approaches included the computation of the difference between the observed and synthesized correlograms but did not yield a more conclusive result or a better resolution.

We compared our estimated shear-wave parameters with some previous estimates (Table 1). At the period T = 1 s and using the PREM parametric form, the shear-wave speed is 3.42 ± 0.02 km/s at the inner core boundary and 3.58 ± 0.02 km/s in the center of Earth. These values are in reasonable agreement with normal mode estimates and with some previous estimates from body-wave observations (Table 1). From these values and the relationship between the shear-wave speed and shear modulus and density, we derived the shear modulus of 149.0 ± 1.6 GPa at the inner core boundary and 167.4 ± 1.6 GPa in the center of Earth. If the compressional speed is taken from PREM (*8*), we can infer the inner core Poisson's ratio of about 0.45. The reduction from the inner core boundary (0.449) to the center (0.444) is smaller than what we can reliably determine with our current precision. In addition, we simulated the amplitudes in the observed correlogram by changing the shear attenuation or the quality factor (Q_μ, an inverse of shear attenuation) in the inner core (fig. S5). This yielded an interval of values for Q_μ, ranging from the PREM values down to the 50% reduction relative to PREM for the idealized and unrealistic extreme case in which the synthetic experiment does not capture the true effects of attenuation. The effect of changing the shear-wave speed and Q structure of the inner core on the inner-core sensitive modes (when the full coupling theory is considered) can be substantial and must be accounted for in resolving the existing normal mode theory-observation misfits. This is in addition to Earth's heterogeneous structure and anisotropy. Eigenfrequencies and Q values of the modes can be strongly affected, and some modes can even exchange their identity (*18*). Our newly estimated shear-wave speed reduction of 2.5% with respect to the PREM model and a hypothetical reduction of 25% in Q_μ would lower the eigenfrequency of the ${}_{10}S_2$ mode by about 3%.

One hypothesis proposed to explain the high attenuation and low shear-wave speed is inner core melt pockets (*19*–*21*). However, although compaction during solidification constrains the upper limit of volume fraction (*22*), theoretical considerations otherwise leave this value unconstrained. A melt volume fraction of more than 10% (*23*) explains the inner core seismological parameters reported in PREM (*8*). Following the same line of argument, our values likely require an even higher portion of melt. Thin films of melt might be consistent with our parameters as the geometry and distribution of melt also affects the shear and attenuation properties.

The hypothesis that premelting effects are prominent near the inner core boundary (*24*) makes determining whether the shear-wave speed reduction occurs only in the top or in the bulk of the inner core relevant. We experimented with the shear-wave speed profiles in Earth's inner core to determine whether we could simulate the timing of the *I2-PKJKP* cusp equally well by reducing the shear-wave speed only in the uppermost part of the inner core. We found that a shear-wave speed reduction of ~35% with respect to the PREM model confined to the uppermost 50 km of the inner core can explain the timing of the *I2-PKJKP* cusp (*14*). However, apart from making the *I2-PKJKP* cusp too weak, this substantial reduction in shear-wave speed cannot predict the correlation phase *PKIIKP-PKIKP* (labeled in supplementary animation S3 and in Fig. 2C), which is a prominent feature in our observed and the best-fit simulated correlograms (Fig. 3). Additionally, *PKIIKP* waves have been observed and their amplitudes studied in conjunction with the shear-wave speed properties of the inner core (*25*). On the basis of this simulation, we thus eliminated the possibility that the shear-wave speed reduction is necessary only in the uppermost inner core. The bulk of the inner core is required to have a reduced shear-wave speed of 2.5% on average. A radial variation of the shear-wave speed is possible, but the exact distribution is hampered by the resolution combined with the non-uniqueness of the problem.

In contrast to the hypotheses above, intrinsic properties of polycrystalline iron at high pressures and temperatures have been proposed to explain the properties of the inner core (*26*, *27*). The ab initio estimates of inner core shear-wave speed (*23*) are 30% larger than the seismological observations. However, when ab initio molecular dynamics calculations account for the shear-wave reducing effects of polycrystallinity, defects, and grain boundaries, they become much more similar to the seismological values. The diffusion of body-centered cubic phase of iron atoms in solid state has been proposed to explain low shear modulus (*28*). Although this study is based on calculations for pure iron, the diffusion mechanism makes the

Table 1. Summary of previous and current results. Shear-wave speed and rigidity of the inner core from different seismological studies. "ICB" indicates measurements at the inner core boundary, and "center" indicates measurements at the center of Earth. For the shear-wave speed data, values that do not have these labels are average values for the inner core in which the shear-wave speed was not explicitly parameterized in terms of Earth's radius. Blank cells indicate that shear-wave speed and rigidity were not explicitly determined in those studies.

Study and method	Shear-wave speed at T = 1 s (km/s)	Rigidity (shear modulus) (GPa)
Dziewonski and Anderson (1981) (*8*)	ICB: 3.4629	ICB: 156.7
Global Earth model PREM	Center: 3.6245	Center: 176.1
Kennett *et al*. (1995) (*36*)	ICB: 3.504	ICB: 156.0
Global Earth model ak135	Center: 3.668	Center: 175.1
Julian *et al*. (1972) (*3*)	2.95 ± 0.1	
Short period body waves	3.62 (reinterpreted) (*4*)	
Wookey and Helffrich (2008) (*7*)	Similar to PREM	
Short period body waves		
Okal and Cansi (1998) (*4*)	3.65	
Intermediate period body waves		
Cao *et al*. (2005) (*6*)	~1.5% faster than that for PREM	
Intermediate period body waves		
Deuss *et al*. (2000) (*5*)	3.6	
Long-period body waves		
This study	ICB: 3.42 ± 0.02	ICB: 149.0 ± 1.6
Earthquake coda cross-correlation	Center: 3.58 ± 0.02	Center: 167.4 ± 1.6

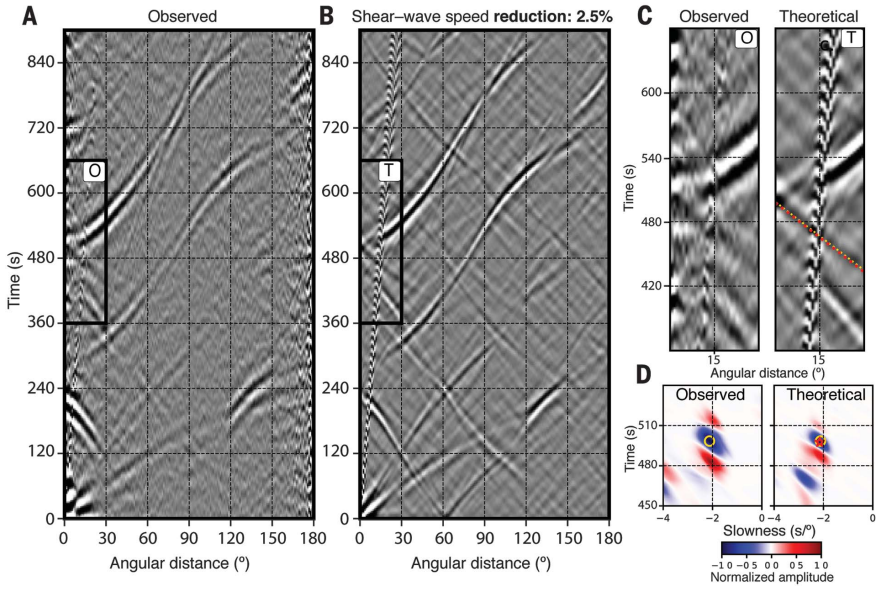

Fig. 3. Observed and synthetic correlograms and the *I2-PKJKP* cusp. (**A** and **B**) A comparison between (A) the observed global correlogram and (B) the best-fit simulated global correlogram for the central period of 23.1 s. The best-fit simulation uses the PREM model with shear-wave speed in the bulk of the inner core reduced by 2.5% [we used a smooth parameter-space search, best viewed as an animation (*14*)]. Compare with the cusp positions in Fig. 2. (**C**) Enlargements of windows O (observed) and T (theoretical) in (A) and (B), focused on the *I2-PKJKP* cusp. (**D**) The observed and simulated (theoretical) slant stacks. The yellow circle corresponds to the lower branch of the *I2-PKJKP* cusp in the slowness-time domain, and the yellow dotted line corresponds to the same in the travel-time domain. The red star in (D) and red dotted line in (C) are the values based on the best-fit Earth model with the 2.5% reduction of shear-wave speed in the inner core.

inner core soft with a very low resistance to shear without requiring the existence of trapped melt to explain seismological observations. Although our study does not exclude any of the above possibilities, it provides seismological evidence for a soft inner core (a less stiff inner core, in terms of its elastic behavior) from a different class of observations.

The relationship between our seismically obtained shear-wave speed and the viscosity is not straightforward. Viscosity depends both on material properties and the dynamics. The mineral physics estimates of viscosity (*29*) are lower than the geodynamic ones (*30*). The mineralogical models generally do not include the effects of microstructures (*31*), which may account for the discrepancy. Our values are consistent with a soft inner core. A dynamically soft core helps explain the lack of gravitational torque–driven length-of-day changes that would be expected with a rigid core combined with the fluctuation in rotation speed inferred from core flow and seismological detection of core rotation (*13*). Moreover, a soft inner core allows for deformation in both the polar and equatorial directions, consistent with observations related to polar motion or nutations (*32*).

Addition of data from local and regional networks will increase the number of station pairs at short angular distances and thus improve the quality of the global correlogram (fig. S1B). Further proliferation of seismic recorders in remote areas of Earth will increase the number of station pairs at antipodal distances. This, in turn, will improve the estimates of the time and amplitude of *J* phase–related features. Determining the frequency dependence of shear wave speeds will also place more constraints on attenuation and viscosity in the inner core. We expect that a shift toward higher frequencies is possible by considering early coda time windows in which the seismic phases are relatively less attenuated owing to their shorter paths through Earth. Detection of *J* waves confirms that Earth's inner core is solid, although elastically less stiff than previous estimates. This inference represents an advance in our understanding of structure and dynamics of the inner core—Earth's deepest time capsule that has been probed by the global correlation wavefield.

REFERENCES AND NOTES

1. I. Lehman, *Publications du Bureau Central séismologique international* **A14**, 87–115 (1936).
2. A. F. Birch, *Am. J. Sci.* **238**, 192–211 (1940).
3. B. R. Julian, D. Davies, R. M. Sheppard, *Nature* **235**, 317–318 (1972).
4. E. A. Okal, Y. Cansi, *Earth Planet. Sci. Lett.* **164**, 23–30 (1998).
5. A. Deuss, J. H. Woodhouse, H. Paulssen, J. Trampert, *Geophys. J. Int.* **142**, 67–73 (2000).
6. A. Cao, B. Romanowicz, N. Takeuchi, *Science* **308**, 1453–1455 (2005).
7. J. Wookey, G. Helffrich, *Nature* **454**, 873–876 (2008).
8. A. M. Dziewonski, D. L. Anderson, *Phys. Earth Planet. Inter.* **25**, 297–356 (1981).
9. A. M. Dziewonski, F. Gilbert, *Nature* **234**, 465–466 (1971).
10. P. M. Shearer, C. A. Rychert, Q. Liu, *Geophys. J. Int.* **185**, 1379–1383 (2011).
11. T.-S. Phạm, H. Tkalčić, M. Sambridge, B. L. N. Kennett, *Geophys. Res. Lett.* **45**, 3035–3042 (2018).
12. R. Deguen, *Earth Planet. Sci. Lett.* **333–334**, 211–225 (2012).
13. H. Tkalčić, *The Earth's Inner Core: Revealed by Observational Seismology* (Cambridge Univ. Press, 2017).
14. Materials and methods are available as supplementary materials.
15. C. Sens-Schönfelder, R. Snieder, S. C. Stähler, *Geophys. Res. Lett.* **42**, 7483–7489 (2015).
16. P. Boué, P. Poli, M. Campillo, P. Roux, *Earth Planet. Sci. Lett.* **391**, 137–145 (2014).
17. H. Kanamori, D. L. Anderson, *Rev. Geophys.* **15**, 105–112 (1977).
18. J. Andrews, A. Deuss, J. Woodhouse, *Geophys. J. Int.* **167**, 204–212 (2006).
19. D. J. Doornbos, *Geophys. J. Int.* **38**, 397–415 (1974).
20. D. R. Fearn, D. E. Loper, P. H. Roberts, *Nature* **292**, 232–233 (1981).
21. S. C. Singh, M. A. Taylor, J. P. Montagner, *Science* **287**, 2471–2474 (2000).
22. I. Sumita, S. Yoshida, M. Kumazawa, Y. Hamano, *Geophys. J. Int.* **124**, 502–524 (1996).
23. L. Vočadlo, in *New Frontiers in Integrated Solid Earth Sciences*, S. A. P. L. Cloetingh, J. Negendank, Eds. (Springer, 2009), pp. 397–412.
24. B. Martorell, L. Vočadlo, J. Brodholt, I. G. Wood, *Science* **342**, 466–468 (2013).
25. V. F. Cormier, *Geophys. Res. Lett.* **42**, 7459–7466 (2015).
26. I. Jackson, J. D. Fitz Gerald, H. Kokkonen, *J. Geophys. Res. Solid Earth* **105**, 23605–23634 (2000).
27. A. B. Belonoshko *et al.*, *Science* **316**, 1603–1605 (2007).
28. A. B. Belonoshko *et al.*, *Nat. Geosci.* **10**, 312–316 (2017).
29. J. A. Van Orman, *Geophys. Res. Lett.* **31**, L20606 (2004).
30. B. A. Buffett, *Nature* **388**, 571–573 (1997).
31. M. I. Bergman, J. Yu, D. J. Lewis, G. K. Parker, *J. Geophys. Res. Solid Earth* **123**, 189–203 (2018).
32. L. Koot, M. Dumberry, *Earth Planet. Sci. Lett.* **308**, 343–349 (2011).
33. Data are available from the IRIS/IDA Seismic Network (https://doi.org/10.7914/SN/II), operated by the Scripps Institution of Oceanography.
34. Data are available from the Global Seismograph Network (https://doi.org/10.7914/SN/IU), operated by the Albuquerque Seismological Laboratory and the USGS.
35. Data are available from the Australian National Seismograph Network (www.fdsn.org/networks/detail/AU/), operated by Geoscience Australia.
36. B. L. N. Kennett, E. R. Engdahl, R. Buland, *Geophys. J. Int.* **122**, 108–124 (1995).

ACKNOWLEDGMENTS

The authors thank three anonymous reviewers for their constructive suggestions on how to improve the manuscript. H.T. is grateful to J. Badro, A. Belonoshko, M. Bergman, G. Helffrich, J. Hernlund, M. Dumberry, I. Jackson, S.-I. Karato, and S. Pachhai for useful discussions. **Funding:** The synthetic experiment was performed on the ANU Terrawulf cluster, a computational facility developed with support from the AuScope initiative. AuScope Ltd. is funded under the National Collaborative Research Infrastructure Strategy (NCRIS), an Australian Commonwealth Government Program. H.T.'s travel was partially supported through the AuScope Excellence in Research Achievement travel bursary award. **Author contributions:** H.T. conceived and supervised the study. Both authors discussed the results and determined the course of the study based on methodological developments achieved during T.-S.P.'s Ph.D. work. The codes for data processing, figures, and data analysis were produced by T.-S.P.; and data analysis and modeling were undertaken by T.-S. P., initiated by and in consultation with H.T., as a part of T.-S.P.'s Ph.D. work. H.T. wrote the manuscript with some edits provided by T.-S.P., edited figures and supplementary material, and interpreted the results in the context of current intellectual framework surrounding the inner core research. **Competing interests:** The authors declare no competing interests. **Data and materials availability:** The facilities of IRIS Data Services, and specifically the IRIS Data Management Center, were used for access to waveforms, related metadata, and/or derived products used in this study. Waveform data used in this study are available from (*33–35*).

SUPPLEMENTARY MATERIALS

www.sciencemag.org/content/362/6412/329/suppl/DC1
Materials and Methods
Figs. S1 to S5
References (*37–45*)
Animations S1 to S3

13 July 2018; accepted 10 September 2018
10.1126/science.aau7649

Science

Shear properties of Earth's inner core constrained by a detection of *J* waves in global correlation wavefield

Hrvoje Tkalcic and Thanh-Son Ph?m

Science **362** (6412), 329-332.
DOI: 10.1126/science.aau7649

A solid and squishy inner core

Earth's inner core is thought to be solid, which means it should support shear waves. However, the small size of the inner core makes detecting shear waves very difficult. Tkalcic and Ph?m correlated different types of seismic phases to finally determine the speed of shear waves in Earth's inner core (see the Perspective by Irving). The detection of the waves closes an 80-year quest to find them and confirms a solid, but soft, inner core.

Science, this issue p. 329; see also p. 294